HHS Public Access

Author manuscript

Circulation. Author manuscript; available in PMC 2024 January 24.

Published in final edited form as:

Circulation. 2023 January 24; 147(4): 324–337. doi:10.1161/CIRCULATIONAHA.122.059346.

RNA-binding protein LIN28a regulates new myocyte formation in the heart via lncRNA-H19

Vagner Oliveira Carvalho Rigaud, PhD[1], **Robert Hoy, MS**[1], **Justin Kurian, MS**[1], **Clare Zarka, BS**[1], **Michael Behanan, BS**[1], **Isabella Brosious, BS**[1], **Jen Pennise, BS**[1], **Tej Patel, BS**[1], **Tao Wang, PhD**[2], **Jaslyn Johnson, PhD**[2], **Lindsay Kraus, PhD**[2], **Sadia Mohsin, PhD**[2], **Steven Houser, PhD**[2], **Mohsin Khan, PhD**[*,1,3]

[1]Center for Metabolic Disease Research, Lewis Katz School of Medicine, Temple University, Philadelphia, PA

[2]Center for Cardiovascular Research, Lewis Katz School of Medicine, Temple University, Philadelphia, PA

[3]Department of Cardiovascular Sciences, Lewis Katz School of Medicine, Temple, University, Philadelphia, PA

Abstract

Background: Developmental cardiac tissue holds remarkable capacity to regenerate after injury and consists of regenerative mononuclear and diploid cardiomyocytes (MNDCMs). Upon maturation, MNDCMs become binucleated or polyploid and exit the cell cycle. Interestingly, cardiomyocyte (CM) metabolism undergoes a profound shift that coincides with cessation of regeneration in the postnatal heart. However, whether reprogramming metabolism promotes persistence of regenerative MNDCMs enhancing cardiac function and repair after injury is unknown. Here, we identify a novel role for RNA-binding protein LIN28a, a master regulator of cellular metabolism, in cardiac repair following injury.

Methods: LIN28a overexpression was tested using mouse transgenesis on postnatal CM numbers, cell cycle and response to apical resection (AR) injury. Using, neonatal and adult cell culture system and adult and MADM myocardial injury models in mice, effect of LIN28a overexpression on cardiomyocyte cell cycle and metabolism was tested. Finally, isolated adult CMs from LIN28a and wildtype mice 4 days after myocardial injury, were used for RNA-immunoprecipitation sequencing (RIP-seq).

Results: LIN28a was found as primarily active during cardiac development and rapidly decreases after birth. LIN28a reintroduction at P1, P3, P5, and P7 decreased maturation-associated

[*]Corresponding author: Mohsin Khan, PhD, Assistant Professor, Center for Metabolic Disease Research, Assistant Professor, Department of Cardiovascular Sciences, Lewis Katz School of Medicine, Temple University, 3500 N Broad Street, MERB 454, Philadelphia, PA, 19140, Phone: 215-707-1921.

Disclosures

None

Supplemental Materials

Supplemental Methods

Supplemental Table S1–S2

Supplemental Figure S1–S9

polyploidization, nucleation, and cell size, enhancing CM cell cycle activity in LIN28a transgenic pups compared to WT littermates. Moreover, LIN28a overexpression extended CM cell cycle activity beyond P7 concurrent with increased cardiac function 30 days after AR. In the adult heart, LIN28a overexpression attenuated CM apoptosis, enhanced cell cycle activity, cardiac function, and survival in mice 12 weeks after myocardial infarction compared to WT littermate controls. Alternatively, LIN28a small molecule inhibitor attenuated pro-reparative effects of LIN28a on the heart. Mechanistically, Neonatal rat ventricular myocytes (NRVMs) overexpressing LIN28a showed increased glycolysis, ATP production and levels of metabolic enzymes compared to control. LIN28a immunoprecipitation followed by RNA sequencing (RIPseq) in CMs isolated from LIN28a-overexpressing hearts after injury identified lncRNA-H19 as its most significantly altered target. Ablation of lncRNA-H19 blunted LIN28a-induced enhancement on CM metabolism and cell cycle activity.

Conclusion: Collectively, LIN28a reprograms CM metabolism and promotes persistence of MNDCMs in the injured heart enhancing pro-reparative processes thereby linking CM metabolism to regulation of ploidy/nucleation and repair in the heart.

Keywords

RNA-binding proteins; cardiac regeneration; cardiomyocyte proliferation; metabolism; ploidy

INTRODUCTION

Developmental cardiac tissue is a proliferative organ capable of regenerating following injury. Cardiomyocytes (CMs) rely on glycolysis for rapid ATP production designed to support increases in cell number in the heart during development[1,2]. Upon cardiac maturation, CMs undergo metabolic changes shifting energy production to fatty-acid oxidation, coinciding with cell cycle exit and loss of cardiac regenerative ability[1]. As a result, strategies based on reprogramming CM metabolism have shown recently to promote cell cycle activity and cardiac repair suggesting a possible connection between metabolic control of CM cell cycle re-entry[3–7]. Similarly, reactivation of developmental signaling in the heart after injury has been effective in augmenting cardiac structure and function[8]. Thus, identification of developmental metabolic regulators of CM polyploidization and multinucleation may provide a novel strategy to restore cardiac repair potential in the adult heart after injury.

During embryonic development, all CMs are mononuclear and diploid (MNDCMs)[9,10] able to actively proliferate and exhibit specialized metabolism. After birth, MNDCMs become binucleated or polyploid that coincides with alteration of metabolism and loss of proliferative capability in the heart[10,11]. Persistence of a small population of MNDCMs in the adult heart has prompted strategies targeting activation of MNDCMs to induce myocardial repair following injury[12–14]. Previously, we have shown that reintroduction of the embryonic stem cell miR-294 in injured adult hearts leads to significant increase in cardiac structure and function, at least in part, by upregulating the RNA-binding protein LIN28a[15]. Unlike other proliferative factors, LIN28a is unique in its ability to regulate multiple cellular processes controlling cellular growth, proliferation, and maturation[16]. Furthermore, LIN28a has been described as a master regulator of metabolism binding

directly to mRNAs of metabolic enzymes as well as repressing let-7 family of microRNAs, a known regulator of CM maturation, cell size, and force contractility[17]. Interestingly, LIN28a expression is lost in adult tissues during development while its reintroduction leads to reprogramming cellular bioenergetics into a juvenile state thereby enhancing organ repair and regeneration[18]. However, the effect of LIN28a in CM proliferation and heart repair after injury is still unknown.

In this study, we explore the therapeutic efficacy of LIN28a as a target for enhancing cardiac structure and function after myocardial injury. We found LIN28a rapidly decreases during heart development and its reintroduction in postnatal mice and in adult injured hearts enhances CM cell cycle activity, and persistence of MNDCMs leading to improved cardiac structure and function after injury. Our results here provide a novel role for RNA-binding protein LIN28a in regulating new myocyte formation in the heart after injury.

METHODS

The authors declare that all supporting data are available within the article and its online supplementary files. Please refer to supplemental methods for an expanded methodology.

Animal Studies

All mice used in this study were obtained from The Jackson Laboratories (Bar Harbor, ME). All procedures and animal care protocols were approved by Temple University Animal Care and Use Committee and performed according to its guidelines in a randomized blinded manner. Please see supplemental methods for expanded experimental setup.

Statistical Analysis

All data sets were assessed for data distribution using Shapiro-Wilk test for normality. For data exhibiting normal distribution, unpaired Student's *t* test was applied when comparing 2 groups, 2-way ANOVA with Sidak post-hoc test for multiple comparison when comparing more than 2 groups, or 2-way mixed effect ANOVA with Geisser-Greenhouse and Tukey corrections when comparing paired data from more than 2 groups. For data not exhibiting normal distribution, Mann-Whitney test or Kruskal-Wallis test with Dunn's correction for multiple comparisons was used. Correlations were performed using Spearman rank correlation test for each group in separately. Kalpan-Meier curves were compared using Mantel-cox test. $P < 0.05$ was considered statistically significant. Error bars represent ±SD. Statistical analysis was performed using Graph Pad prism v 9.0 software.

RESULTS

LIN28a defines CM numbers in the postnatal heart.

Developmental heart consists of dividing cardiomyocytes (CMs) that exit the cell cycle shortly after birth. To test whether LIN28a plays a role in regulating CM cell cycle during postnatal heart development, we first analyzed the expression of LIN28a in developing (P1, P3, P5, and P7) and adult wild type (WT) hearts (P60). Results show LIN28a was highly expressed at P1 but rapidly decreases within the first week of life, coinciding with

the loss of proliferative window in CMs upon maturation and is almost absent during adulthood (Figure 1A). Next, we utilized transgenic mice that overexpress LIN28a in all organs of the body including the heart and CMs (Supplementary Figure 1A–D), and have been shown as a model to study organ regeneration[18]. LIN28a overexpressing pups showed increased body and heart weights but no change in heart/body weight ratio and baseline cardiac function (Supplemental Figure 1M), indicating proportionate increase in heart size without hypertrophy or atrophy (Supplementary Figure 1E–H). Hearts were isolated from LIN28a and WT littermates during postnatal heart development (Figure 1B) to assess CM cell cycle activity. LIN28a overexpressing pups showed increased Ki67+ and pHH3+ CMs (Figure 1C–D) at P1, P3, P5 and P7 together with enhanced mRNA levels of cell cycle genes (Supplemental Figure 1J–K). Analysis of cytokinesis marker AurB showed increased expression in LIN28a pups (Figure 1E) concurrent with significant increase (15.1%) in total number of CMs counted per field at P7 only compared to WT animals (Figure 1F) suggesting that early increase in Ki67/pHH3+ CMs manifests into increases in cytokinetic CMs by P7. We further confirmed these findings by digesting LIN28a-overexpressing and WT hearts at P7 followed by CM isolation and analysis of cell cycle markers. Concurrent with histological analysis, isolated CMs from P7 LIN28a hearts showed a 3.4-fold increase in pHH3 levels (Figure 1G). We next sought to determine whether LIN28a reintroduction could extend the cell cycle activity in postnatal CMs beyond P7. To test this, we compared the hearts of LIN28a overexpressing pups and WT littermates at P14, one week after the end of the proliferative window. Interestingly, LIN28a overexpressing pups showed continued increase in AurB+ CMs (3.0-fold) and expression of cell cycle genes (Figure 1H; Supplemental Figure 1L), along with 12.5% more total number of CMs per field (Figure 1I). Total CM numbers were further assessed by isolating cardiomyocytes at P7, 14 and P60 and showed significantly increased CMs/heart compared to WT littermates (Supplementary Figure 1I). In summary, by using in vitro and in vivo approaches, we demonstrate that LIN28a overexpression during postnatal heart development enhances CM cell cycle activity and CM numbers at least up to two weeks after birth.

LIN28a is required for neonatal heart regeneration and its overexpression extends regenerative window.

As LIN28a pups demonstrate increased cell cycle activity in CMs at P7, we hypothesized LIN28a may extend cardiac regenerative ability. To test this hypothesis, we performed apical resection (AR) in LIN28a-overexpressing pups and their WT littermates at P7, when the heart is largely composed of cell cycle arrested CMs (Figure 2A). Hearts were isolated 4 days after AR from both groups of animals followed by immunohistochemistry analysis that showed a 2.5-fold increase in pHH3+ CMs in LIN28a-overexpressing pups (Figure 2B) and increased CMs per field (Figure 2C) compared to WT pups with AR suggesting LIN28a promotes cell cycle activity even in the injured P7 heart. Speckle-tracking based strain and LV-trace echocardiography analysis revealed enhanced cardiac function 30 days after AR with increased global and apical longitudinal strain and rates (GLS, ALS; 16.3% and 26.2%, respectively) in LIN28a pups compared to control (Figure 2D–E, Supplemental Figure 2A–C). No changes in heart rate were observed during the measurements (Supplemental Figure 2D). Left ventricular ejection fraction (Figure 2F), and fractional shortening (Supplemental Figure 2E–F) was significantly enhanced (28.6%/WT and 20.5%/WT respectively) together

with reduced systolic volume and diameter (Supplemental Figure 2G–H). Masson's trichrome staining identified significant scar formation in the apex of the WT hearts that was completely abrogated in LIN28a-overexpressing pups 30 days after AR (Figure 2G).

To test whether loss of LIN28a alters transient cardiac regenerative ability of the P1 heart, we first determined whether LIN28a is altered in the postnatal heart after apical resection. Results showed that P1 hearts of WT pups with AR show significant increase in LIN28a expression 7 days post AR compared to uninjured littermates (Figure 2H) suggesting LIN28a may play a role in the maintenance of postnatal cardiac regenerative potential. Neonatal rat ventricular myocytes (NRVMs) from P1 WT rat pups were isolated and treated with LIN28a1632 (called here as LIN28a inhibitor), a potent small molecule that inhibits LIN28a binding to let-7 pre-micro-RNA[19]. LIN28a RNA levels were significantly reduced after inhibitor treatment together with a 0.21-fold decrease in pHH3+ CMs (Supplemental Figure 3A–C) suggesting LIN28a is essential for neonatal CM cell cycle activity. To confirm this hypothesis, we performed AR on P1 WT pups followed by intraperitoneal (IP) injections of 25mg/kg LIN28a inhibitor or PBS for 3 consecutive days and collection of hearts at 7- and 30-days post resection (7dpr and 30dpr; Figure 2I). At 7dpr, mRNA levels of LIN28a were found to be decreased in hearts of pups treated with LIN28a inhibitor, validating the treatment (Supplemental Figure 4A). In line with our *in vitro* data, LIN28a inhibition significantly reduced CM cell cycle activity as represented by a reduction of 2.7-fold in pHH3+ CMs (Figure 2J) and expression of cell cycle genes (Supplemental Figure 4B) at 7dpr. Furthermore, LIN28a-inhibitor treated pups exhibited reduced cardiac structure and function 30 days after injury as analyzed by speckle-tracking based 3D regional wall velocity and vector diagrams (Supplemental Figure 4C–G). A reduction of 27.4% in left ventricular ejection fraction (EF; Figure 2K), and fractional shortening (FS; Supplemental Figure 4H) and enhanced LVIDs (Supplemental Figure 4I) were also observed in LIN28a-inhibitor treated pups compared to non-treated animals at 30dpr. Concurrently, LIN28a inhibitor treatment increased heart weight to body weight ratio suggesting myocardial hypertrophy (Supplemental Figure 4J–K) compared to non-treated animals at 30dpr. Collectively, our data suggests that LIN28a is essential for preservation and extension of the transient cardiac regenerative potential of the murine heart.

LIN28a promotes persistence of mononucleated, diploid CMs in the heart during postnatal development and injury.

The postnatal heart contains a distinct regenerative subpopulation of mononucleated and diploid cardiomyocytes (MNDCMs) that become polyploid and multinucleated with cardiac maturation[10], coinciding with loss of regenerative ability. Interestingly, the persistence of MNDCMs in the adult heart is associated with better outcome after injury[12]. Since LIN28a reintroduction enhances pro-regenerative processes in the postnatal heart, we hypothesized that LIN28a may promotes persistence of MNDCMs. To test it, we stained postnatal hearts during first week after birth with CM-specific nuclear membrane marker Pericentriolar Material 1 (PCM1) and wheat germ agglutinin (WGA; Figure 3A). By measuring the cross area of PCM1+ CMs, we observed that LIN28a-overexpressing hearts are comprised of smaller CMs when compared to their WT littermates that becomes significant at P3 (Figure 3B). Concurrently, LIN28a-overexpressing hearts showed a higher % of mononucleated

CMs as determined by the number of PCM1+ nuclei per longitudinal CMs (Figure 3C). This difference in nucleation becomes even more pronounced from P5-P14 in the LIN28a pups when typically, CMs exhibit a mature phenotype and exit the cell cycle. Additionally, we determined the DNA content of the CMs by comparing DAPI intensity of PCM1+ CMs to PCM1-non-myocyte nuclei using MATLAB software and z-stack imaging. Remarkably, decreased ploidy levels in CMs from LIN28a-overexpressing pups were observed in all time points from P3 compared to WT littermates (Figure 3D). Further analysis showed increased % of diploid CMs in LIN28a-overexpressing hearts (Figure 3E) compared to WT littermates at P3, P5, and P7.

To determine whether LIN28a promotes similar persistence of MNDCMs after cardiac injury, we reassessed WT and LIN28a-overexpressing hearts after resection (Figure 3F) for cell size, nucleation, and ploidy levels. Consistent with previous results, CMs from LIN28a-overexpressing hearts were 14.8% smaller in size, 12.5% more mononucleated and showed 46.6% less ploidy levels, 30 days post resection (Figure 3G–I, respectively). Interestingly, the % of mononucleated CMs per mouse strongly correlated ($r=0.8032$; $p=0.0296$ for WT and $r=0.7642$; $p=0.0455$ for LIN28a) with their respective cardiac function 30 days after AR suggesting amount or persistence of mononucleated CMs in the LIN28a overexpressing hearts is associated to better cardiac functional recovery after injury (Figure 3J).

LIN28a enhances CM cell cycle activity by reprogramming metabolism.

We recognize that LIN28a transgenic mice express the protein globally and the effects on CM proliferation may be in part dependent upon crosstalk with other cardiac cells. Therefore, to characterize proliferative effects of LIN28a specifically in the CMs, we synthesized an adenovirus for LIN28a under the CM specific promoter cTnT. NRVMs were isolated from P1–2 wild type (WT) rats and treated with either LIN28a-adenovirus with a GFP tag or GFP only-adenovirus as a control (Supplemental Figure 5A–B). Reintroduction of LIN28a in NRVMs significantly increased cell cycle activity showing a 2.1-fold increase in Ki67+, 4.2-fold in EdU+, 1.95-fold in pHH3+, and 1.58-fold in AurB+ CMs (Figure 4A–D), along with enhanced expression of cell cycle genes (Supplemental Figure 5C) compared to controls 48hrs post transduction. As an alternative visualization of the data, Euler plots were generated (right panels of Figure 4A–D) showing the total numbers of analyzed cells (white) for every marker/treatment, number of actinin+ CMs (gray), GFP+ CMs (blue), and Ki67/EdU/pHH3/AurB+ CMs (red). One of the main features of immature CMs is high glycolytic rate. With maturation, CM metabolism shifts towards a oxidative state coinciding with polyploidization, multinucleation, and cell cycle-arrest[9,11]. To determine whether LIN28a alters CM metabolic processes, we analyzed the glycolytic and oxidative fluxes of NRVMs overexpressing LIN28a or GFP adenoviruses using Seahorse Bioanalyzer. Glycolysis stress test revealed increased extracellular acidification rate (ECAR; Figure 4E–F) and glycolytic capacity in LIN28a treated NRVMs together with enhanced mRNA levels of glycolytic enzymes (Supplemental Figure 6A), increased lactate production (Figure 4G) along with higher pyruvate kinase activity (Figure 4H). Conversely, mitochondrial stress test showed a reduction in oxygen consumption rate (OCR), decreased maximal respiration, and spare respiratory capacity in LIN28a-overexpressing NRVMs compared to control cells (Supplemental Figure 6B–D). Decreased citrate synthase activity

(Supplemental Figure 6E) and mitochondrial DNA content (Supplemental Figure 6F) in NRVMs-LIN28a further assessed mitochondrial activity. This reduction in oxidative phosphorylation (OxPhos), however, did not result in reduced energy production as measured by total ATP content (Supplemental Figure 6G). Next, we tested whether blocking glycolysis or OxPHOS with 2-deoxy-d-Glucose (2-DG) or antimycin A (AA) respectively, alters LIN28a ability to change CM cell cycle activity. Remarkably, blocking glycolysis completely abrogated the pro-proliferative effect of LIN28a reducing % of pHH3+ CMs (Figure 4I) while inhibition of OxPhos does not seems to significantly blunt salutary effect of LIN28a on pHH3 levels (Supplemental Figure 6H). The main question was whether LIN28a induced metabolic changes are differentially manifested in mono vs binucleated CMs. Analysis of mitochondrial membrane potential, a key indicator of mitochondrial activity, revealed an overall reduction in NRVMs after LIN28a overexpression compared to controls (Supplemental Figure 6I). However, TMRM intensity was significantly lower in mononucleated LIN28a CMs rather than binucleated cells compared to controls (Figure 4K). Similarly, analysis of mitochondrial ROS in NRVMs-LIN28a showed reduced overall mitochondrial superoxide production as measured by mitoSOX staining (Supplemental Figure 6J) that was significantly lower among the mononucleated CMs with no difference between the binucleated population (Figure 4L). Collectively, our data suggests that LIN28a-induced enhancement in cell cycle activity and persistence of MNDCMs is dependent upon metabolic reprogramming towards glycolysis with mononucleated CMs particularly receptive to LIN28a induced metabolic changes.

LIN28a enhances cardiac structure and function in the adult heart after injury.

The next question is whether LIN28a promotes enhancement of cardiac function in the adult heart. To test this hypothesis, we performed myocardial infarct (MI) in fully mature adult (6 months old) LIN28a overexpressing mice, and their WT littermates followed by serial functional and histological assessments (Figure 5A). Remarkably, LIN28a overexpressing mice showed significantly enhanced survival (Figure 5B) than their WT littermates (hazard ratio 0.1998, 95% CI of ratio 0.04739 to 0.8421). LIN28a mice also presented increased left ventricle function with improved ejection fraction (Figure 5C, Supplemental Figure 7A) and fractional shortening (Figure 5D) 12 weeks after MI when compared to controls together with an increase in left ventricle anterior wall thickness (LVAW; Supplemental Figure 7B) and reduction in internal diameter (LVID; Supplemental Figure 7C). No difference in heart rate was observed during echocardiography (Supplemental Figure 7D). Additionally, speckle-tracking based strain analysis on echocardiography B-mode loops was performed revealing significant improvement in apical and longitudinal strain and rates in LIN28a overexpressing mice compared to controls 12 weeks post MI (Figure 5E–I). Furthermore, hemodynamic measurement showed increased cardiac contractility in LIN28a hearts compared to their WT littermates 12 weeks post MI (Figure 5J–L). In parallel, LIN28a hearts showed 9.6% less infarcted area at 12 weeks post MI (Figure 5M) and decrease in apoptosis 2 days after injury (Supplemental Figure 7E). Additional body organ weights to body weight ratios did not change in both groups of mice (Supplemental Figure 7F–I).

LIN28a enhances CM cell cycle activity in the adult heart after myocardial infarction injury.

To test whether LIN28a enhances adult CM cell cycle activity, we first utilized adult feline CMs (AFM) due to their ability to survive long term in culture as described previously[15] and transduced with adenoviruses carrying GFP-tagged LIN28a or GFP only as a control (Supplemental Figure 8A). Analysis of LIN28a overexpressing AFM showed reduced cell size (Supplemental Figure 8B), increased % of mononucleated AFMs (Supplemental Figure 8C) and reduced ploidy levels (Supplemental Figure 8D) together with a 3.3-fold increase in pHH3+ AFMs (Supplementary Figure 8E). However, the main question was whether LIN28a promotes CM cell cycle activity in the adult heart after injury. To answer this question, we utilized dual pulse-chase labeling based on EdU administration in the first week and BrdU in the second week to LIN28a overexpressing and control mice after MI (Figure 5A). At 4 weeks after injury, 9.9% of the CMs were labeled with EdU in LIN28a overexpressing hearts compared to 4.3% in the WT controls (Figure 6A), a 2.3-fold increase in EdU+ CM in LIN28a hearts (Figure 6C). In addition, 3.8% of the CMs in LIN28a hearts were labeled with both EdU and BrdU compared to 1.0% in the WT controls, suggesting CMs that incorporated EdU during the first week after injury continued undergoing cell cycle through the second week after MI (3.6-fold increase) (Figure 6A and C). At 12 weeks, a 2.2-fold increase in EdU+CMs (11.3% LIN28a vs. 5.2% WT), 4.1-fold in dual EdU/BrdU+ CMs (9.9% LIN28a vs. 2.5% WT), and 1.3-fold in BrdU+ CMs (18.7% LIN28a vs. 13.8% WT) incorporations were observed in LIN28a hearts compared to controls. Furthermore, LIN28a overexpressing mice also presented 1.5 and 1.8-fold increase in pHH3+ CMs at 4 and 12 weeks, respectively, when compared to their WT littermates (Figure 6B). Changes in cell cycle activity in LIN28a-overexpressing mice at 4 and 12 weeks after injury are summarized in Figure 6C. EdU labeling of CMs was further confirmed by digesting whole hearts for single EdU+ CMs and showed LIN28a significantly increased EdU+ CMs compared to controls 12 weeks after MI (Figure 6D). Additionally, LIN28a hearts consisted of significantly smaller CMs (Figure 6E–F) and increased mononucleated CMs (Figure 6G) with decreased ploidy levels (Figure 6H), consistent with a reduced heart to body weight ratio (Supplemental Figure 8F). The persistence of mononucleated CMs in adult mice showed moderate to strong correlation ($r=0.6606$; $p=0.0438$) with their respective cardiac function 12 weeks after MI suggesting LIN28a-induced persistence of mononucleated CMs could provide a better reparative response to injury (Figure 6J). Although LIN28a promotes the persistence of mononucleated CMs, we did not observe higher LIN28a levels in mononucleated CMs when compared to binucleated CMs isolated from adult LIN28a-overexpressing mice (Supplemental Figure 8G). Concurrently, LIN28a hearts showed increased expression of LIN28a at 4 and 12 weeks (Supplementary Figure 8H) together with enhanced glycolytic gene expression (Supplementary Figure 8I) 4 weeks after MI in contrast to WT animals that have minimal LIN28a at baseline, completely abrogated 4 days after MI (Supplementary Figure 8J). As a proof of concept, we suppressed glycolytic metabolism in infarcted LIN28a-overexpressing mice by systemic delivery of 100mg/Kg 2-DG administered at the time of MI and daily thereafter. Adult CMs were then isolated 4 days after injury and assessed for metabolism and cell cycle activity. Consistent with our previous results, 2-DG treatment blunted LIN28a-induced enhancement in glycolysis, as measured by seahorse glycolysis stress test, and cell cycle activity, as measured by immunocytochemistry of cell cycle marker Ki67

(Supplemental Figure 8K and L). Finally, we utilized CM-specific Mosaic Analysis with Double Markers (MADM) mouse model to determine CMs that undergo complete cell cycle through cytokinesis allowing unambiguous identification of newly generated CMs. Adeno-associated virus serotype 9 (AAV9) carrying LIN28a or control were retro-orbitally delivered to MADM mice followed by induction of MI. Two weeks after injury, hearts were digested and CMs were isolated for determination of single-color CMs (Figure 6K). Interestingly, animals receiving AAV9-LIN28a showed a 1.9 and 1.5-fold increase in GFP and RFP, respectively, single-labeled CMs when compared to controls suggesting LIN28a overexpression enhances generation of new CMs. Taken together, our results suggest that LIN28a enhances CM cell cycle activity and persistence of MNDCMs in adult mice after injury leading to the generation of new regenerative CMs.

Salutary effects of LIN28a are linked to lncRNA-H19 binding in the adult heart after injury.

To provide mechanistic insight into LIN28a salutary effects on cardiac repair, we isolated CMs from adult LIN28a-overexpressing mice 4 days after MI followed by RNA-immunoprecipitation (RIP) to isolate RNAs bound to LIN28a or control IgG and submitted for bulk RNA sequencing (RIPseq; Figure 7A). Analysis showed a total of 42,482 transcripts sequenced and 8516 genes passed the false discovery rate (FDR) filtering (Supplementary Figure 9A) together with distribution of total nucleotide bases in the reads (Figure 7B) 4 days after MI in the LIN28a adult CMs compared to IgG. Differential gene expression analysis (DESeq2) identified 98 genes differentially expressed (DEGs) between LIN28a and control IgG with fold-change >1.5 and padj-value<0.05 with 65 (66.3%) up and 33 (33.7%) downregulated (Figure 7C). A volcano plot representation illustrates the distribution of the 8516 genes highlighting the significant up (green) and downregulated (red) genes with identification of lncRNA-h19 as the top upregulated gene (Figure 7D). Next, a Pearson correlation (Supplemental Figure 9B) and principal component analysis (PCA) (Supplemental Figure 9C) were performed showing consistency within all LIN28a sample datasets and a distinct profile in LIN28a adult CMs when compared to IgG 4 days after MI. For further data visualization and distribution, a heatmap and hierarchical clustering was generated using DEGs dataset highlighting differential expression profile in LIN28a compared to IgG 4 days after MI (Figure 7E). Gene ontology (GO) analysis was performed using PANTHER 16.0 classification system that identified top over-represented terms for biological processes. Interestingly, significant GO terms for LIN28a binding targets included metabolic processes, cell proliferation, and regulation of apoptosis and aging (Figure 7F).

Analysis identified long non-coding RNA H19 (lncRNA-H19) as the most significant and differentially expressed transcript, highly enriched in the LIN28a fraction when compared to control IgG (log2FC = 6.47, padj-value = 3.31×10^{-141}; Figure 7D). Moreover, lncRNA-H19 was found to be the most representative gene in our dataset with an average of 21,640 readings/ sample, 35 times more than the second most represented gene (620 readings; Figure 7G). Next, we confirmed increased lncRNA-H19 expression in NRVMs transduced with LIN28a compared to controls by qPCR (Figure 7H). Concurrently, we found lncRNA-H19 to be increased in LIN28a-overexpressing mice both during postnatal development and after apical resection injury at P1 and P7 (Supplemental Figure 9D–F). Recent work described lncRNA-H19 as a regulator of aerobic glycolysis and proliferation in different

cancer types[20,21]. To test whether LIN28a mediated glycolysis is part dependent upon lncRNA-H19, we knocked-down lncRNA-H19 using small interfering RNAs (siH19) in NRVMs overexpressing LIN28a (Figure 7H) and measured glycolytic flux and cell cycle activity. lncRNA-H19 knock down negatively impacted on LIN28a-induced enhancement of cell cycle activity significantly reducing pHH3 levels by 27.6% (Figure 7I) together with complete reversal of pro-glycolytic effect conferred by LIN28a overexpression as measured by seahorse bioanalyzer (Figure 7J) and mRNA expression of glycolytic enzymes (Supplementary Figure 9I). Taken together, our results suggest that LIN28a mediated enhancement of cardiac structure and function in the adult heart after MI is in part dependent upon lncRNA-H19 targeting of glycolysis required for maintenance of cell cycle activity in CMs.

DISCUSSION

Our findings here identify a novel role for RNA binding protein LIN28a in regulating CM cell cycle activity to define CM numbers in the postnatal heart during development and injury and in the adult heart following myocardial infarction. Additionally, our data identifies LIN28a promotes persistence of mononucleated diploid CMs in the heart associated with increased functional recovery, reprograms CM metabolism towards glycolysis through direct binding to lncRNA H19, a known regulator of aerobic glycolysis and proliferation that together augments cardiac structure and function in the heart after myocardial injury (Figure 7K).

Adult cardiac tissue is largely dormant with less than 1% turnover during the lifetime of an individual[22]. In contrast, early postnatal heart consists of proliferative CMs capable of resolving myocardial injury, however this ability is lost by P7 upon cardiac maturation, changes in cardiac environment and increased functional demand on the heart associated with individual growth. Several strategies based upon microRNAs[15], gain or loss of function for positive and negative regulators of cell cycle[23], hormonal regulation[4], alterations in oxygen levels[2] have been employed to reactivate cell cycle activity in the adult heart. Due to the proliferative nature of the developmental cardiac tissue, studies have utilized reactivation of developmental signaling factors in the adult heart to drive CM proliferation[8]. In this respect, our previous work has identified developmental RNA-binding protein LIN28a for promoting cardiac cell proliferation and survival[24]. LIN28a was first identified in *C.elegans* linked to regulation of developmental timing or heterochrony[25]. Subsequent studies have shown LIN28a to be associated with maintenance of pluripotency[16], cell cycle regulation[16] and delayed differentiation[26]. Zhu and colleagues recently developed LIN28a doxycycline inducible transgenic mice with constitutively low levels of leaky LIN28a expression in the absence of induction[26]. LIN28a overexpression in these mice enhances growth and delays puberty together with increased ability to regenerate injured tissues[18]. Interestingly, authors showed that LIN28a expression is seven-fold higher in the skeletal muscle than wild-type mice but whether this extends to the heart was not tested[18]. Therefore, in the present study we demonstrate that LIN28a transgenic mice exhibit significant changes in CM numbers, cell cycle activity in the postnatal heart and possess ability to regenerate cardiac tissue after injury in accordance with prior literature. Furthermore, we show that LIN28a overexpression

extends transient cardiac regenerative potential of the postnatal heart to P7 in accordance with similar studies[27,28]

An interesting aspect of our findings was the ability of LIN28a to promote persistence of mononuclear diploid CMs (MNDCMs) in the heart during postnatal development, injury and in the adult heart after myocardial damage. CMs are mononuclear and diploid (MNDCMs)[9,10] able to actively proliferate during development becoming binucleated or polyploid and cell cycle arrested after birth [10,11]. Studies recently show existence of small subsets of ventricular and atrial CMs in the adult human heart samples based on unique transcriptional differences in metabolic activity, retinoic acid responsiveness and expression of smooth muscle cell signaling pathways[29,30]. Similarly, 2 independent studies using snRNA-seq described the existence of a rare regenerative CM population (0.4% of total cardiac cells) and regulation of cell cycle in a CM subpopulation by non-coding RNA that suggests presence of CMs with inherent regenerative properties in the adult heart[31,32]. Cui and colleagues showed that the postnatal heart contains a highly proliferative subpopulation of diploid and mononuclear CMs with specialized metabolism[33]. After birth, these CMs become polyploid and multinucleated coinciding with a shift in metabolism, cell cycle-arrest and loss of regeneration. Persistence of a small population of MNDCMs in the adult heart has prompted strategies targeting activation of MNDCMs to induce myocardial repair following injury[12–14]. Another study from last year showed how IGF2 is essential for neonatal heart regeneration via ‘proliferation-competent’ mononuclear diploid CMs[28]. LIN28a is a known regulator of IGF2 enhancing its translation[16,34] and although we didn’t not look at IGF2-LIN28a axis in this study, it further provides support towards LIN28a ability to induce persistence of MNDCMs as observed in our results.

It has been shown recently that cardiac metabolism undergoes a profound shift in the early postnatal heart in response to changes in cardiac environment and maturation. During development, embryonic CMs rapidly proliferate and rely on glycolysis for ATP production[1,2]. As the heart grows, CMs utilize primarily fatty-acid oxidation that coincides with cell cycle exit and loss of regenerative potential[1]. Recent studies implicate CM metabolism as a determinant of cell cycle activity[5,7,35] suggesting manipulation of metabolic pathways including induction of glycolysis as a viable strategy for cardiac regeneration following injury. We have previously shown LIN28a introduction in cardiac cells increases glycolytic metabolites, intermediates and glycolysis linked to enhanced survival and proliferation[24]. Similarly, in this study we show that LIN28a introduction drives glycolytic metabolism and cell cycle activity in CMs while inhibition of glycolysis reverses this phenotype. Mechanistically, results were tied to LIN28a ability to bind and regulate expression of lncRNA-H19 in accordance with previous documented role of LIN28a as an RNA-binding protein. Previous reports show lncRNA-H19 is a potent regulator of aerobic glycolysis and proliferation in various cancer cells[21]. LncRNA-H19 can induce and activate pyruvate kinase muscle isozyme 2 (PKM2), essential for Warburg effect and tumorigenesis[20]. Hypoxia also induces lncRNA-H19 expression that is involved in regulating signal transduction, glucose metabolism and expression of glycolysis gatekeeper pyruvate dehydrogenase kinase 1 (PDK1) in cancer cells[21]. In the heart, lncRNA-H19 expression is known to downregulate in the failing hearts of mice, pigs and humans[36]. Recently, lncRNA-H19 therapy was shown to prevent and reverse cardiac hypertrophy in

trans-aortic (TAC) constriction model of hypertrophy in mice suggesting a therapeutic role for lncRNA-H19 in the heart[36]. Therefore, our findings are in concurrence with these studies and suggest that LIN28a mediated glycolysis and salutary effects on cardiac structure and function may in part be dependent on lncRNA-H19.

In conclusion, our findings here identify a novel role for RNA-binding protein LIN28a in heart during postnatal development and adult heart after injury. LIN28a defines CMs numbers during postnatal development and is critical for the maintenance of transient regenerative potential of the postnatal heart. In the adult heart, LIN28a promotes cell cycle activity and augments cardiac structure and function by reprogramming CM metabolism towards glycolysis dependent upon RNA-binding to lncRNA-H19 after myocardial injury.

Supplementary Material

Refer to Web version on PubMed Central for supplementary material.

Acknowledgments

We thank all members of the Khan laboratory for their valuable discussions as well Temple Flow Cytometry core.

Sources of Funding

This work was supported by National Institute of Health grant HL135177 and American heart Association Transformational Project Award 20TPA35490355 to M. Khan and HL137850 to S. Mohsin. VOC. Rigaud was supported by American Heart Association Postdoctoral Fellowship Award 828777.

List of Non-standard Abbreviations and Acronyms

CM	Cardiomyocytes
MNDCM	Mononuclear diploid cardiomyocytes
EdU	5-ethynyl-2’-deoxyuridine
AurB	Aurora B kinase
TUNEL	Terminal deoxynucleotidyl transferase (TdT)-mediated dUTP nick end labeling
OXPHOS	Oxidative phosphorylaiton
OCR	Oxygen consumption rate
ECAR	Extracellular acidification rate
NRVM	Neonatal rat ventricular myocytes
EF	Ejection fraction
FS	Fractional shortening
LVID	Left ventricular internal diameter
LVAW	Left ventricular anterior wall

AR	Apical resection
RIP-seq	RNA immunoprecipitation sequencing
WGA	Wheat germ agglutinin
MADM	Mosaic analysis with double markers
2-DG	2-deoxy-d-glucose

References

1. de Carvalho A, Bassaneze V, Forni MF, Keusseyan AA, Kowaltowski AJ, Krieger JE. Early Postnatal Cardiomyocyte Proliferation Requires High Oxidative Energy Metabolism. Sci Rep. 2017;7:15434. doi: 10.1038/s41598-017-15656-3 [PubMed: 29133820]
2. Puente BN, Kimura W, Muralidhar SA, Moon J, Amatruda JF, Phelps KL, Grinsfelder D, Rothermel BA, Chen R, Garcia JA, et al. The oxygen-rich postnatal environment induces cardiomyocyte cell-cycle arrest through DNA damage response. Cell. 2014;157:565–579. doi: 10.1016/j.cell.2014.03.032 [PubMed: 24766806]
3. Cardoso AC, Lam NT, Savla JJ, Nakada Y, Pereira AHM, Elnwasany A, Menendez-Montes I, Ensley EL, Petric UB, Sharma G, et al. Mitochondrial Substrate Utilization Regulates Cardiomyocyte Cell Cycle Progression. Nat Metab. 2020;2:167–178. [PubMed: 32617517]
4. Hirose K, Payumo AY, Cutie S, Hoang A, Zhang H, Guyot R, Lunn D, Bigley RB, Yu H, Wang J, et al. Evidence for hormonal control of heart regenerative capacity during endothermy acquisition. Science. 2019;364:184–188. doi: 10.1126/science.aar2038 [PubMed: 30846611]
5. Magadum A, Singh N, Kurian AA, Munir I, Mehmood T, Brown K, Sharkar MTK, Chepurko E, Sassi Y, Oh JG, et al. Pkm2 Regulates Cardiomyocyte Cell Cycle and Promotes Cardiac Regeneration. Circulation. 2020;141:1249–1265. doi: 10.1161/CIRCULATIONAHA.119.043067 [PubMed: 32078387]
6. Fukuda R, Marin-Juez R, El-Sammak H, Beisaw A, Ramadass R, Kuenne C, Guenther S, Konzer A, Bhagwat AM, Graumann J, et al. Stimulation of glycolysis promotes cardiomyocyte proliferation after injury in adult zebrafish. EMBO Rep. 2020;21:e49752. doi: 10.15252/embr.201949752 [PubMed: 32648304]
7. Honkoop H, de Bakker DE, Aharonov A, Kruse F, Shakked A, Nguyen PD, de Heus C, Garric L, Muraro MJ, Shoffner A, et al. Single-cell analysis uncovers that metabolic reprogramming by ErbB2 signaling is essential for cardiomyocyte proliferation in the regenerating heart. Elife. 2019;8. doi: 10.7554/eLife.50163
8. Rigaud VOC, Khan M. Aging in reverse: Reactivating developmental signaling for cardiomyocyte proliferation. J Mol Cell Cardiol. 2021;154:1–5. doi: 10.1016/j.yjmcc.2020.12.017 [PubMed: 33460687]
9. Li F, Wang X, Capasso JM, Gerdes AM. Rapid transition of cardiac myocytes from hyperplasia to hypertrophy during postnatal development. J Mol Cell Cardiol. 1996;28:1737–1746. doi: 10.1006/jmcc.1996.0163 [PubMed: 8877783]
10. Soonpaa MH, Kim KK, Pajak L, Franklin M, Field LJ. Cardiomyocyte DNA synthesis and binucleation during murine development. Am J Physiol. 1996;271:H2183–2189. doi: 10.1152/ajpheart.1996.271.5.H2183 [PubMed: 8945939]
11. Mollova M, Bersell K, Walsh S, Savla J, Das LT, Park SY, Silberstein LE, Dos Remedios CG, Graham D, Colan S, et al. Cardiomyocyte proliferation contributes to heart growth in young humans. Proc Natl Acad Sci U S A. 2013;110:1446–1451. doi: 10.1073/pnas.1214608110 [PubMed: 23302686]
12. Patterson M, Barske L, Van Handel B, Rau CD, Gan P, Sharma A, Parikh S, Denholtz M, Huang Y, Yamaguchi Y, et al. Frequency of mononuclear diploid cardiomyocytes underlies natural variation in heart regeneration. Nat Genet. 2017;49:1346–1353. doi: 10.1038/ng.3929 [PubMed: 28783163]

13. Senyo SE, Steinhauser ML, Pizzimenti CL, Yang VK, Cai L, Wang M, Wu TD, Guerquin-Kern JL, Lechene CP, Lee RT. Mammalian heart renewal by pre-existing cardiomyocytes. Nature. 2013;493:433–436. doi: 10.1038/nature11682 [PubMed: 23222518]

14. Chen X, Wilson RM, Kubo H, Berretta RM, Harris DM, Zhang X, Jaleel N, MacDonnell SM, Bearzi C, Tillmanns J, et al. Adolescent feline heart contains a population of small, proliferative ventricular myocytes with immature physiological properties. Circ Res. 2007;100:536–544. doi: 10.1161/01.RES.0000259560.39234.99 [PubMed: 17272809]

15. Borden A, Kurian J, Nickoloff E, Yang Y, Troupes CD, Ibetti J, Lucchese AM, Gao E, Mohsin S, Koch WJ, et al. Transient Introduction of miR-294 in the Heart Promotes Cardiomyocyte Cell Cycle Reentry After Injury. Circ Res. 2019;125:14–25. doi: 10.1161/CIRCRESAHA.118.314223 [PubMed: 30964391]

16. Peng S, Chen LL, Lei XX, Yang L, Lin H, Carmichael GG, Huang Y. Genome-wide studies reveal that Lin28 enhances the translation of genes important for growth and survival of human embryonic stem cells. Stem Cells. 2011;29:496–504. doi: 10.1002/stem.591 [PubMed: 21425412]

17. Viswanathan SR, Daley GQ, Gregory RI. Selective blockade of microRNA processing by Lin28. Science. 2008;320:97–100. doi: 10.1126/science.1154040 [PubMed: 18292307]

18. Shyh-Chang N, Zhu H, Yvanka de Soysa T, Shinoda G, Seligson MT, Tsanov KM, Nguyen L, Asara JM, Cantley LC, Daley GQ. Lin28 enhances tissue repair by reprogramming cellular metabolism. Cell. 2013;155:778–792. doi: 10.1016/j.cell.2013.09.059 [PubMed: 24209617]

19. Roos M, Pradere U, Ngondo RP, Behera A, Allegrini S, Civenni G, Zagalak JA, Marchand JR, Menzi M, Towbin H, et al. A Small-Molecule Inhibitor of Lin28. ACS Chem Biol. 2016;11:2773–2781. doi: 10.1021/acschembio.6b00232 [PubMed: 27548809]

20. Fan C, Tang Y, Wang J, Xiong F, Guo C, Wang Y, Zhang S, Gong Z, Wei F, Yang L, et al. Role of long non-coding RNAs in glucose metabolism in cancer. Mol Cancer. 2017;16:130. doi: 10.1186/s12943-017-0699-3 [PubMed: 28738810]

21. Peng F, Wang JH, Fan WJ, Meng YT, Li MM, Li TT, Cui B, Wang HF, Zhao Y, An F, et al. Glycolysis gatekeeper PDK1 reprograms breast cancer stem cells under hypoxia. Oncogene. 2018;37:1062–1074. doi: 10.1038/onc.2017.368 [PubMed: 29106390]

22. Bergmann O, Zdunek S, Felker A, Salehpour M, Alkass K, Bernard S, Sjostrom SL, Szewczykowska M, Jackowska T, Dos Remedios C, et al. Dynamics of Cell Generation and Turnover in the Human Heart. Cell. 2015;161:1566–1575. doi: 10.1016/j.cell.2015.05.026 [PubMed: 26073943]

23. Mohamed TMA, Ang YS, Radzinsky E, Zhou P, Huang Y, Elfenbein A, Foley A, Magnitsky S, Srivastava D. Regulation of Cell Cycle to Stimulate Adult Cardiomyocyte Proliferation and Cardiac Regeneration. Cell. 2018;173:104–116 e112. doi: 10.1016/j.cell.2018.02.014 [PubMed: 29502971]

24. Yuko AE, Carvalho Rigaud VO, Kurian J, Lee JH, Kasatkin N, Behanan M, Wang T, Luchesse AM, Mohsin S, Koch WJ, et al. LIN28a induced metabolic and redox regulation promotes cardiac cell survival in the heart after ischemic injury. Redox Biol. 2021;47:102162. doi: 10.1016/j.redox.2021.102162 [PubMed: 34628272]

25. Ambros V, Horvitz HR. Heterochronic mutants of the nematode Caenorhabditis elegans. Science. 1984;226:409–416. doi: 10.1126/science.6494891 [PubMed: 6494891]

26. Zhu H, Shah S, Shyh-Chang N, Shinoda G, Einhorn WS, Viswanathan SR, Takeuchi A, Grasemann C, Rinn JL, Lopez MF, et al. Lin28a transgenic mice manifest size and puberty phenotypes identified in human genetic association studies. Nat Genet. 2010;42:626–630. doi: 10.1038/ng.593 [PubMed: 20512147]

27. Han Z, Wang X, Xu Z, Cao Y, Gong R, Yu Y, Yu Y, Guo X, Liu S, Yu M, et al. ALKBH5 regulates cardiomyocyte proliferation and heart regeneration by demethylating the mRNA of YTHDF1. Theranostics. 2021;11:3000–3016. doi: 10.7150/thno.47354 [PubMed: 33456585]

28. Shen H, Gan P, Wang K, Darehzereshki A, Wang K, Kumar SR, Lien CL, Patterson M, Tao G, Sucov HM. Mononuclear diploid cardiomyocytes support neonatal mouse heart regeneration in response to paracrine IGF2 signaling. Elife. 2020;9. doi: 10.7554/eLife.53071

29. Litvinukova M, Talavera-Lopez C, Maatz H, Reichart D, Worth CL, Lindberg EL, Kanda M, Polanski K, Heinig M, Lee M, et al. Cells of the adult human heart. Nature. 2020;588:466–472. doi: 10.1038/s41586-020-2797-4 [PubMed: 32971526]

30. Marin-Sedeno E, de Morentin XM, Perez-Pomares JM, Gomez-Cabrero D, Ruiz-Villalba A. Understanding the Adult Mammalian Heart at Single-Cell RNA-Seq Resolution. Front Cell Dev Biol. 2021;9:645276. doi: 10.3389/fcell.2021.645276 [PubMed: 34055776]

31. Galow AM, Wolfien M, Muller P, Bartsch M, Brunner RM, Hoeflich A, Wolkenhauer O, David R, Goldammer T. Integrative Cluster Analysis of Whole Hearts Reveals Proliferative Cardiomyocytes in Adult Mice. Cells. 2020;9. doi: 10.3390/cells9051144 [PubMed: 33375150]

32. Tabula Muris C, Overall c, Logistical c, Organ c, processing, Library p, sequencing, Computational data a, Cell type a, Writing g, et al. Single-cell transcriptomics of 20 mouse organs creates a Tabula Muris. Nature. 2018;562:367–372. doi: 10.1038/s41586-018-0590-4 [PubMed: 30283141]

33. Cui M, Wang Z, Chen K, Shah AM, Tan W, Duan L, Sanchez-Ortiz E, Li H, Xu L, Liu N, et al. Dynamic Transcriptional Responses to Injury of Regenerative and Non-regenerative Cardiomyocytes Revealed by Single-Nucleus RNA Sequencing. Dev Cell. 2020;55:665–667. doi: 10.1016/j.devcel.2020.11.006 [PubMed: 33290696]

34. Zhu H, Shyh-Chang N, Segre AV, Shinoda G, Shah SP, Einhorn WS, Takeuchi A, Engreitz JM, Hagan JP, Kharas MG, et al. The Lin28/let-7 axis regulates glucose metabolism. Cell. 2011;147:81–94. doi: 10.1016/j.cell.2011.08.033 [PubMed: 21962509]

35. Fukuda R, Marin-Juez R, El-Sammak H, Beisaw A, Ramadass R, Kuenne C, Guenther S, Konzer A, Bhagwat AM, Graumann J, et al. Stimulation of glycolysis promotes cardiomyocyte proliferation after injury in adult zebrafish. 2020:e49752. doi: 10.15252/embr.201949752

36. Viereck J, Buhrke A, Foinquinos A, Chatterjee S, Kleeberger JA, Xiao K, Janssen-Peters H, Batkai S, Ramanujam D, Kraft T, et al. Targeting muscle-enriched long non-coding RNA H19 reverses pathological cardiac hypertrophy. Eur Heart J. 2020;41:3462–3474. doi: 10.1093/eurheartj/ehaa519 [PubMed: 32657324]

Clinical Perspective

What is new?

- For the first time, a role for RNA-binding protein LIN28a in regulating cardiomyocyte turnover in the postnatal and adult heart has been documented.
- LIN28a overexpression promotes CM cell cycle activity during postnatal development and extends cardiac regenerative ability of the mammalian heart to postnatal day 7. In the adult heart, LIN28a drives new myocyte formation augmenting cardiac structure and function after myocardial injury.
- Mechanistically, LIN28a induces metabolic reprogramming via binding and regulating expression of lncRNA-H19 and is associated with increased persistence of mononuclear diploid cardiomyocytes in the adult heart after injury.

What are the clinical implications?

- This study provides a novel translational role for LIN28a based strategy to replenish cardiomyocytes in the adult heart after injury.
- These findings will enable development of strategies in the future for reintroduction of ‘developmental metabolic factors’ that promote regeneration in the adult heart after injury.

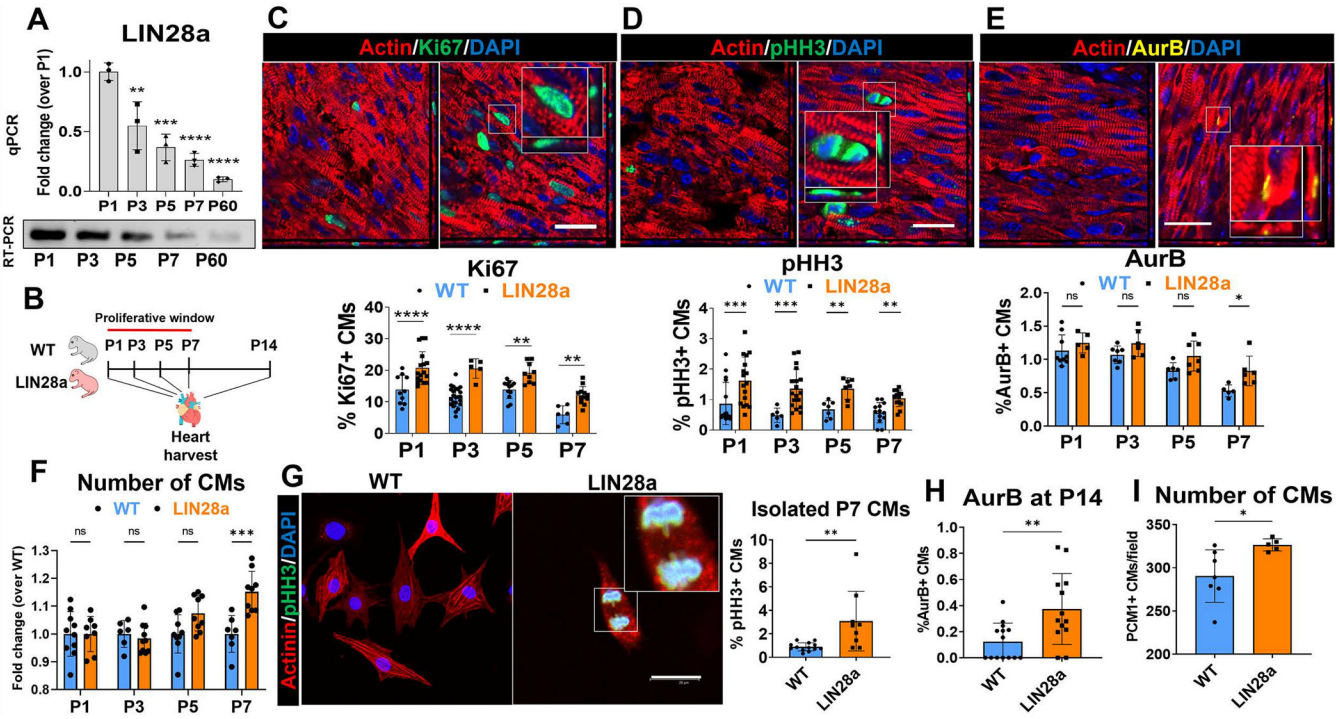

Figure 1: LIN28a regulates CM cell activity and number in the heart during postnatal development.

A) LIN28a mRNA expression levels decrease after birth (n=5 animals per time point). B) Schematic illustration of the experimental design. C-E) Immunohistochemistry (IHC) analysis of 3 cell cycle markers (Ki67, pHH3, and AurB) in postnatal hearts of LIN28a-overexpressing pups compared to their WT littermates along with quantification. Red = alpha-sarcomeric actin, Green = Ki67/pHH3, AurB = yellow, Blue = nuclei; scale bar 40μM; n = 6 animals per time point. F) Number of PCM1+ cross sectioned CMs per field in postnatal hearts from LIN28a-overexpressing pups and their WT littermates at P1, P3, P5 and P7. Images stained for WGA, PCM1 and DAPI; n= 6 animals per time point. Values were normalized over WT littermates. G) Analysis of pHH3+ CMs isolated from P7 hearts of LIN28a-overexpressing pups and WT controls. Red = alpha-sarcomeric actinin, Green = pHH3, Blue = nucleus; n= 4 animals per group. H) Analysis of the cytokinetic maker AurB in P14 hearts from LIN28a and WT pups. n= 6 animals. I) Number of PCM1+ cross sectioned CMs per field in P14 hearts from LIN28a and WT controls. Images stained for WGA, PCM1 and DAPI; n= 6 animals. Data from A was analyzed using Kruskal-Wallis test with Dunn's correction for multiple comparisons; from C-F, 2way ANOVA with Sidak correction for multiple comparisons was applied; from H-I, Mann-Whitney test was applied. Control/WT vs. LIN28a *p<0.05, **p<0.01, ***p<0.001, ****p<0.0001.

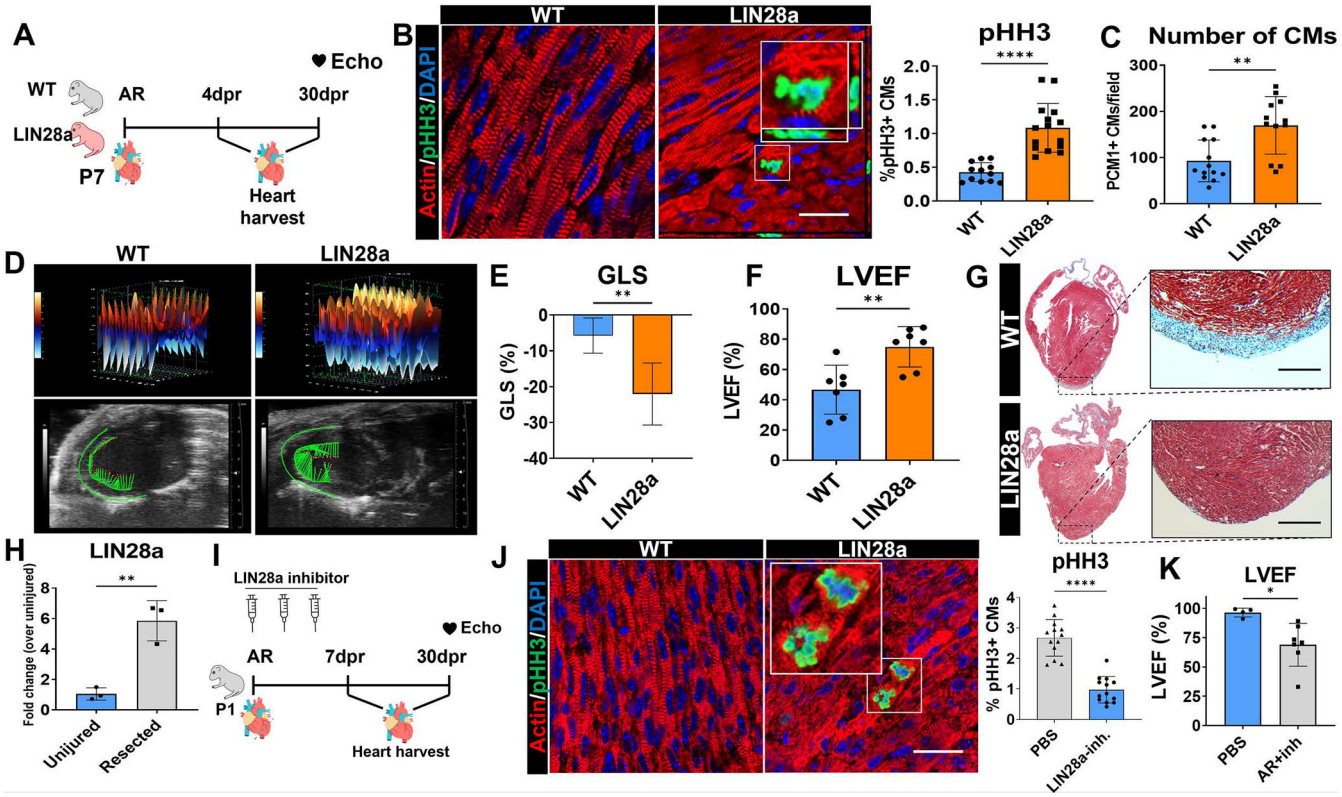

Figure 2: LIN28a is required for neonatal heart regeneration and its overexpression extends regenerative window.

A) Schematic illustration of the experimental design. B) Analysis of pHH3+ CMs in resected P7 hearts of LIN28a-overexpressing pups and WT controls 4 days after injury. Red = alpha-sarcomeric actin, Green = pHH3, Blue = nuclei; n=6 animals. Scale bar=20μM C) Number of PCM1+ cross sectioned CMs per field in resected P7 hearts from LIN28a-overexpressing pups and their WT littermates 30 days after injury. Images stained for WGA, PCM1 and DAPI; n=6 animals per time point. D-E) Speckle-tracking based analysis of B-mode echocardiography images showing enhanced Global Longitudinal Strain (GLS) in resected P7 LIN28a hearts compared to WT controls 30 days after injury. n=7 animals per group. F) Enhanced left ventricular ejection fraction (LVEF) in resected P7 LIN28a hearts compared to WT controls 30 days after injury measured by LV tracing of M-mode echocardiography images. n=7 animals per group. G) Masson's trichome staining showing reduced formation of scar tissue in the resected apex of LIN28a heart compared to WT control. Red = muscle fibers, Blue = collagen. Scale bar=100μM H) mRNA levels of LIN28a are increased in resected P1 WT hearts 7 days after injury compared to uninjured P8 WT pups measured by qPCR. N=3 animals per group. I) Schematic illustration of the experimental plan. J) Analysis of pHH3=CMs showing cell cycle activity is decreased in resected P1 WT pups treated with 3 injections of LIN28a inhibitor compared to their littermates treated with PBS 7 days after injury. Red=alpha-sarcomeric actin, Green = pHH3, Blue = nuclei; n = 6 animals/group. Scale bar=20μM K) LVEF is reduced in resected P1 WT hearts treated with LIN28a inhibitor compared to controls treated with PBS 30 days after injury as measured by LV tracing in M-mode echocardiography images. n=7 animals per

group. Data from B-G and I-K was analyzed using Mann-Whitney test; for H, unpaired t-test was applied. WT vs. LIN28a or Uninjured vs. Resected or PBS vs. LIN28a-inh. *p<0.05, **p<0.01, ***p<0.001, ****p<0.0001.

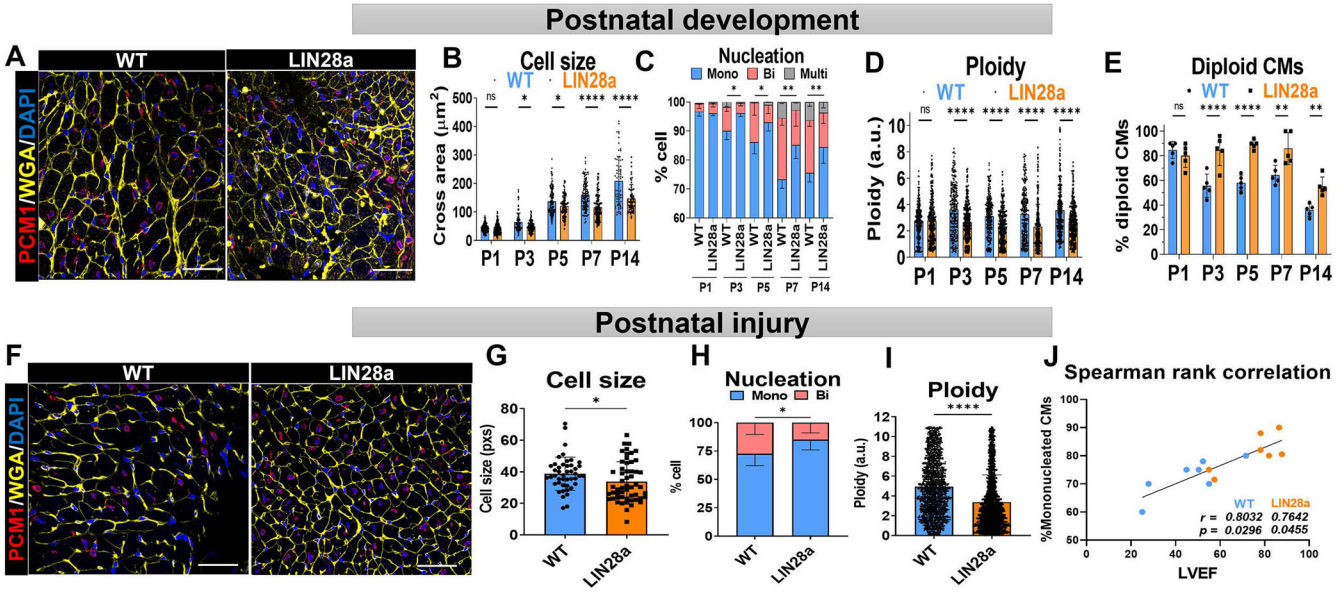

Figure 3: LIN28a induced persistence of mononucleated and diploid CMs is associated with enhanced functional recovery.

A) Representative images of WGA (yellow) and PCM1 (red) staining in the postnatal heart showing CM cross-section area. Scale bar=40μM B) LIN28a overexpressing pups showed decreased cell size compared to their WT littermates starting from P3. Cell size calculated as cross-sectional area; n=6 animals. C) % of mononucleated CMs is increased in LIN28a overexpressing pups compared to controls starting from P3. Number of nuclei was calculated based on PCM1 staining in longitudinally oriented CMs by MATLAB; n=6 animals. D) Ploidy levels are reduced in LIN28a overexpressing pups compared to their WT littermates. Ploidy was calculated in an automated manner based on intensity of DAPI in PCM1+ nuclei compared to a non-myocyte (PCM1-) in the same field. a.u.=arbitrary unit; n=6 animals. E) LIN28a overexpressing mice showed increased % of diploid CMs compared to WT controls. % of diploid CMs was calculated manually in longitudinally oriented CMs based on the intensity of DAPI in PCM1+ nuclei compared to a non-myocyte (PCM1-) in the same field. F) Representative images of WGA (yellow) and PCM1 (red) staining showing CM cross-sectional area in P7 LIN28a overexpressing and WT hearts 30 days after apical resection. Scale bar=40μM G) CMs from P7 LIN28a overexpressing pups showed smaller cell size compared to their WT littermates 30 days after resection. Cell size calculated as cross-sectional area; n=6 animals. H) % of mononucleated CMs is increased in P7 LIN28a overexpressing heart compared to the controls 30 days after resection. Number of nuclei was calculated based on PCM1 staining in longitudinally oriented CMs; n=6 animals. I) CMs from P7 LIN28a overexpressing hearts have decreased ploidy levels compared to their WT littermates 30 days after resection. Ploidy was calculated in an automated manner based on intensity of DAPI in PCM1+ nuclei compared to a non-myocyte (PCM1-) in the same field. a.u. = arbitrary unit; n=6 animals. J) Spearman rank correlation showing strong association between % of mononucleated CMs and left ventricle ejection fraction 30 days after injury. % of mononucleated CMs were calculated for every mouse by averaging nucleation data from 6 different images followed by correlation to their paired LVEF values; n=14 animals. LIN28a-overexpressing pups=orange, WT littermates=blue.

Data from B-E and H was analyzed using 2way ANOVA with Sidak correction for multiple comparisons; for G and I unpaired Student's t test was applied; for J, Spearman rank correlation was performed for each group in separately. WT vs. LIN28a *p<0.05, **p<0.01, ***p<0.001, ****p<0.0001.

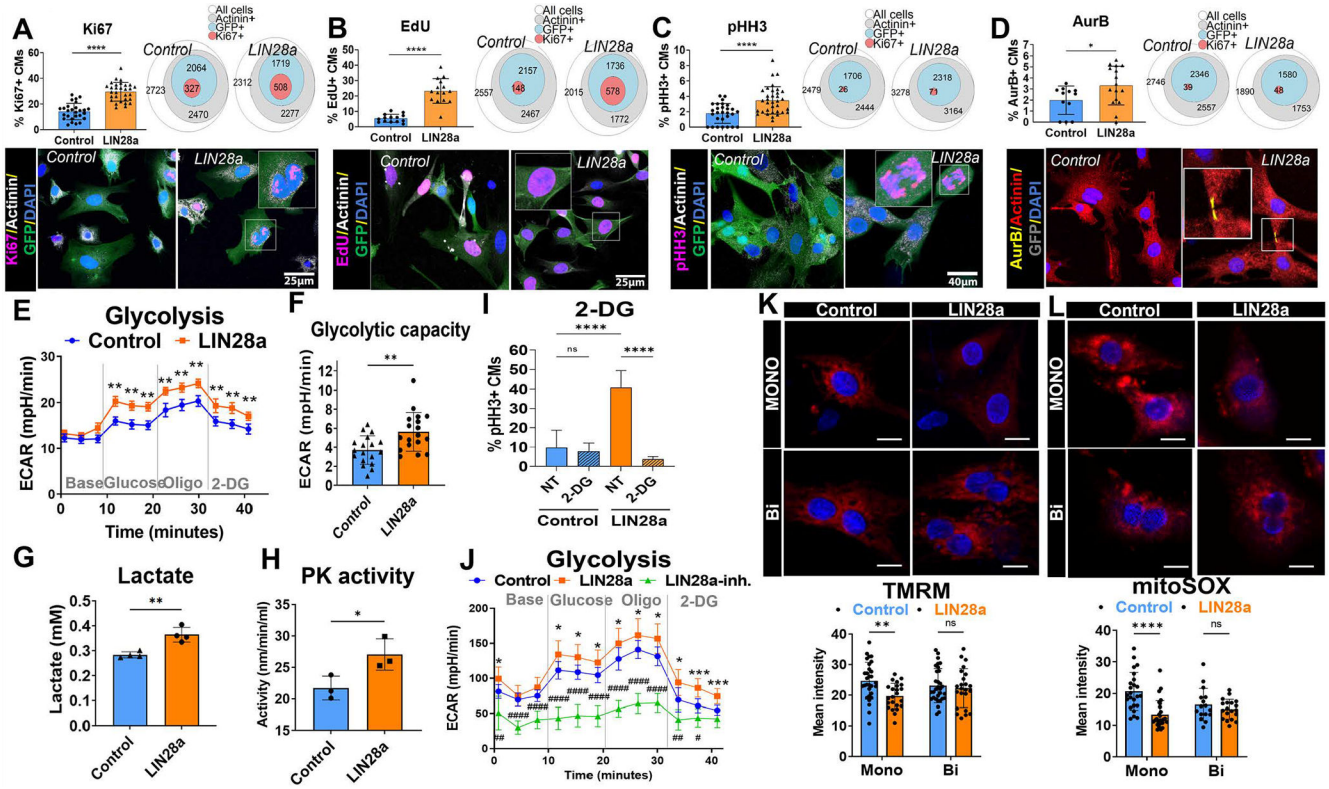

Figure 4: LIN28a reprograms CM metabolism to enhance cell cycle activity.

A-D) Analysis of cell cycle markers (Ki67, EdU incorporation, pHH3, and AurB) in NRVMs 48h after transduction with adenoviruses overexpressing GFP-tagged LIN28a or GFP only as control. Purple=Ki67/EdU/pHH3, yellow=AurB, White=alpha-sarcomeric actinin, Green or gray=GFP, Blue=nuclei; scale bar=25μM in A, B, and 40μM in C, D; Euler plots represent the number of +cells for each condition analyzed using MATLAB software; White circle=total number of cells counted under each treatment, grey circle=actinin+ cells, blue circle=GFP+ cells and red circle=Ki67/EdU/pHH3/AurB+ cells. n=4 different experiments. E-F) Seahorse glycolysis stress test revealed enhanced glycolytic flux and glycolytic capacity in NRVMs 48h after transduction with adenoviruses overexpressing LIN28a compared to controls. n=3 independent experiments, 12 technical replicates per experiment. G-H) Lactate production and pyruvate kinase (PK) activity are enhanced in NRVMs 48h after transduction with adenoviruses overexpressing LIN28a compared to controls. n=4 and 3 independent experiments, respectively. I) Analysis of pHH3 revealed decreased cell cycle activity in NRVMs overexpressing LIN28a after treatment with 50mM 2-Deoxy-d-Glucose (2-DG) for 24h. n=4 independent experiments; Red=cardiac troponin T, Green=pHH3, Gray=GFP, Blue=nuclei. J) Decreased glycolysis in LIN28a-NRMVs in the presence of small molecule LIN28a inhibitor as measured by seahorse assay. n=3 independent experiments, 12 technical replicates/group/experiment. K-L) Mitochondrial membrane potential and superoxide production are decreased in mononucleated, but not binucleated NRVMs 48h after transduction with adenoviruses overexpressing LIN28a compared to controls as measured by TMRM and mitoSOX staining (Red), respectively. Scale bar=20μM. n=5 independent experiments. Data from A-D, F, and G was analyzed

using Mann-Whitney test; for H, unpaired t-test was applied; for E and J, 2way mixed effect ANOVA with Geisser-Greenhouse and Tukey corrections was applied; for I Kruskal-Wallis test with Dunn's correction for multiple comparisons was applied; .for K and L, 2way ANOVA with Sidak correction for multiple comparisons was applied. Control vs. LIN28a *p<0.05, **p<0.01, ***p<0.001, ****p<0.0001.

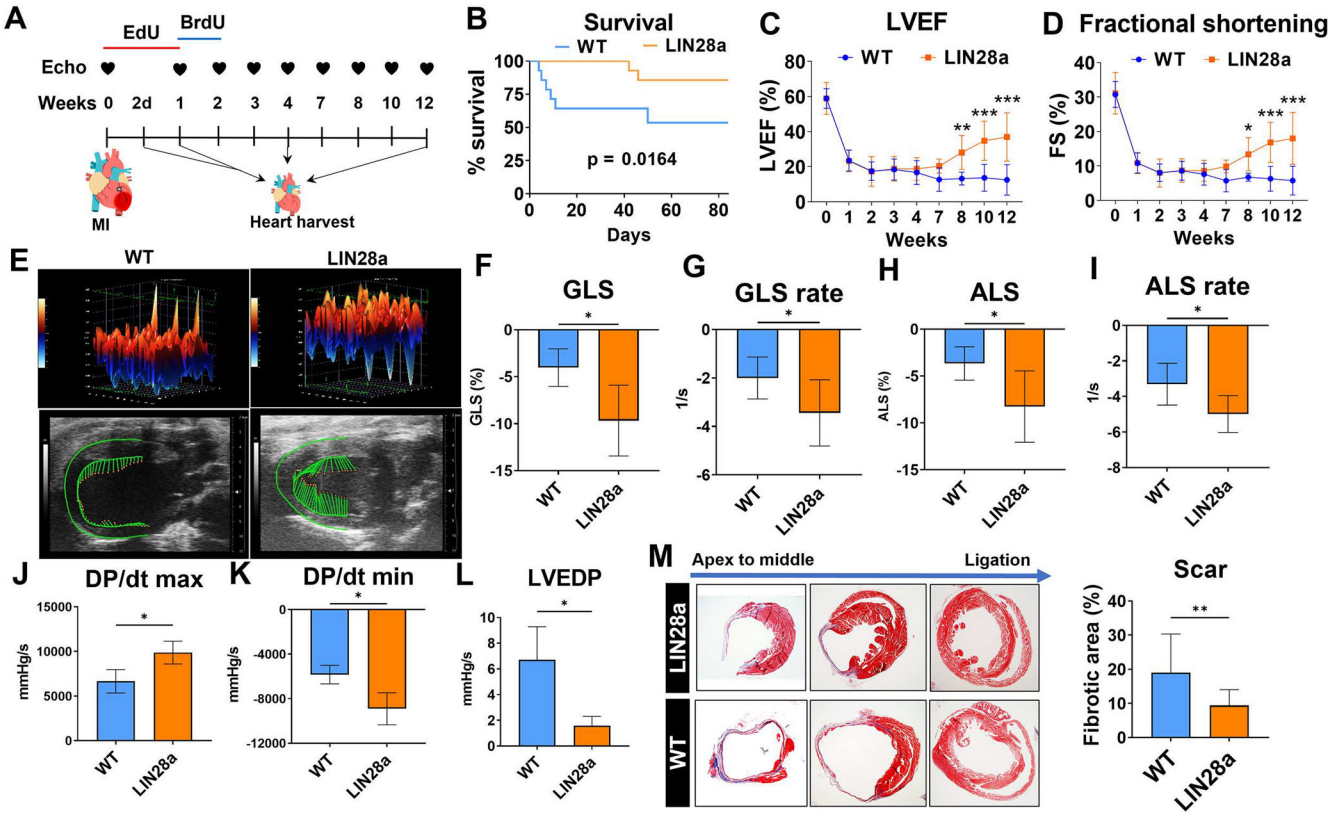

Figure 5: LIN28a augments cardiac structure and function after myocardial infarction in adult mice.

A) Schematic illustration of the experimental design. B) Kaplan-Meier survival curve showing transgenic mice overexpressing LIN28a have enhanced survival up to 84 days (12 weeks) after myocardial infarct (MI) when compared to their WT littermates. n=17 animals per group. C-D) Left ventricle trace analysis of M-mode echocardiography images revealed LIN28a-overexpressing mice have enhanced cardiac function 12 weeks after MI as evidenced by increased left ventricle ejection fraction (LVEF) and fractional shortening (FS) levels. n=17 animals per group. E-I) Speckle tracking analysis of B-mode images revealed improved cardiac systolic function in LIN28a-overexpressing mice compared to WT controls 12 weeks after MI as evidenced by enhanced global and apical longitudinal strains and rates (GLS, GLS rate, ALS, and ALS rate). n=17 animals per group. J-L) Hemodynamic measurements showing improved heart function in LIN28a-overexpressing mice compared to WT controls 12 weeks after MI. n=4 animals per group. M) Masson's trichome staining in hearts showing reduced infarct size in transgenic mice overexpressing LIN28a compared to their WT littermates 12 weeks after MI. n=8 animals per group. Kalpan-Meier curves were analyzed using Mantel-cox test; for C and D, 2way mixed effect ANOVA with Geisser-Greenhouse and Tukey corrections was applied; for F-M Mann-Whitney test was applied. WT vs. LIN28a *p<0.05, **p<0.01, ***p<0.001, ****p<0.0001.

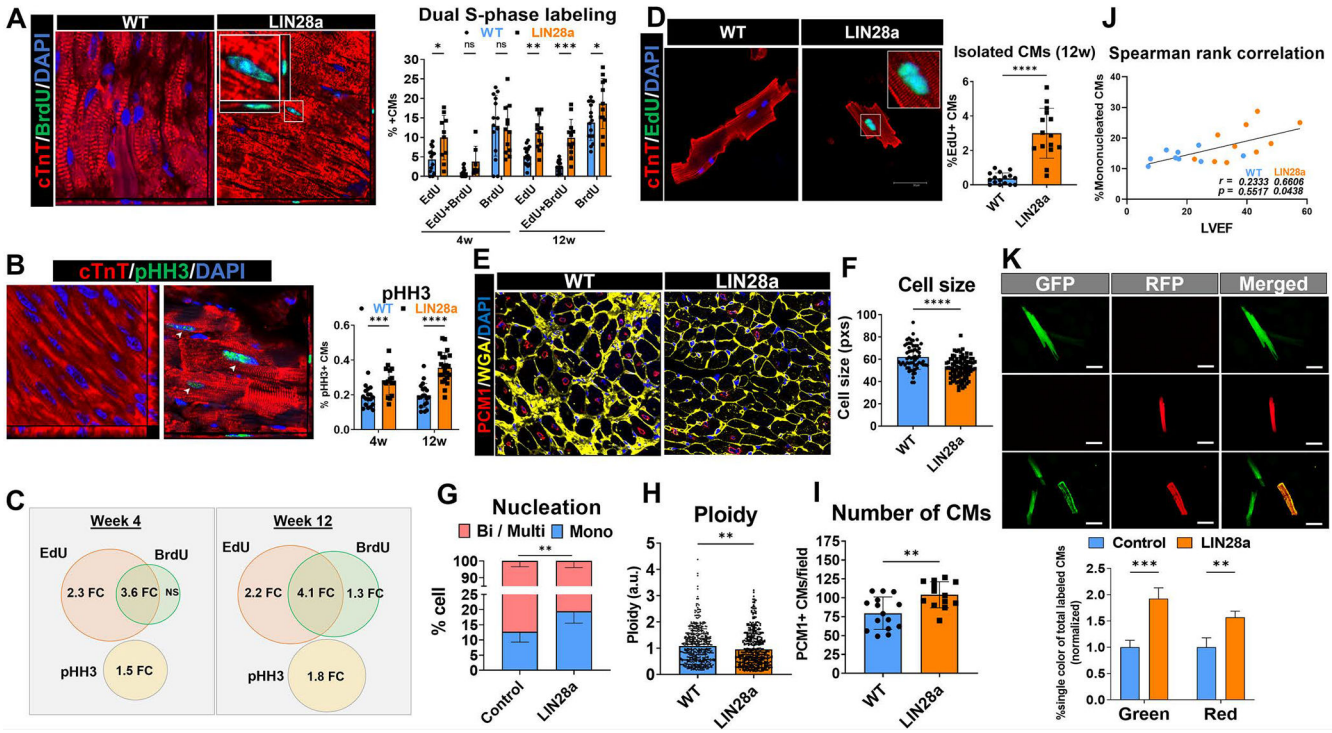

Figure 6: LIN28a promotes CM cell cycle activity and new myocyte formation in the adult heart after injury.

A) S-phase dual labeling with EdU and BrdU in hearts sections from LIN28a and WT mice 4 and 12 weeks after MI for quantification for single EdU+, BrdU+ or double EdU/BrdU+ CMs. n=6 independent experiments; Red=cardiac troponin T, Green=EdU/BrdU, and Blue=nuclei; scale bar=50μM. B) Analysis of pHH3 showing enhanced CM cell cycle activity in LIN28a mice 4 and 12 weeks after MI when compared to WT controls. n=6 independent experiments; Red=cardiac troponin T, Green=pHH3, and Blue=nuclei; scale bar=70μM. C) Euler diagram representing changes in CM cell cycle activity in LIN28a-overexpressing mice compared to WT controls in different time points after injury. D) EdU labeling and detection in isolated adult CMs from hearts from LIN28a overexpressing and control mice 12 weeks after MI. Red=cardiac troponin T, Green=EdU and Blue=nuclei; scale bar=20μM. E-F) Representative image and quantification of WGA images showing CMs from LIN28a overexpressing mice have smaller cell size compared to their WT littermates 12 weeks after MI. Cell size calculated as cross area; n=6 animals. WGA = yellow, PCM1 = red, Nuclei = blue. scale bar=70μM. Nucleation (G) and ploidy levels (H) are reduced in LIN28a mice compared to WT 12 weeks after MI. a.u.=arbitrary unit; n=6 animals. I) LIN28a-overexpressing mice have enhanced number of PCM1+ CMs per filed compared to their WT counterparts 12 weeks after MI. n=6 independent experiments. J) Spearman rank correlation showing association between percentage of mononucleated CMs and left ventricle ejection fraction 12 weeks after injury. Percentages of mononucleated CMs were calculated for every mouse by averaging nucleation data from 6 different z-stack images followed by correlation to their paired LVEF values. n=19 animals. LIN28a-overexpressing mice=orange, WT littermates=blue. K) Representative immunofluorescence images and quantification of single-colored (red or green) CMs isolated from α-MHC

Mer-Cre-Mer MADM mice, indicating newly generated CMs that underwent cytokinesis. n=5 animals per group. Data from A, B, G, and K was analyzed using 2way ANOVA with Sidak correction for multiple comparisons; for D and I, Mann-Whitney test was applied. For F, and H, unpaired t test with Welch's correction was applied; for J, Spearman rank correlation was performed for each group in separately. Control vs. LIN28a or WT vs. LIN28a *p<0.05, **p<0.01, ***p<0.001, ****p<0.0001.

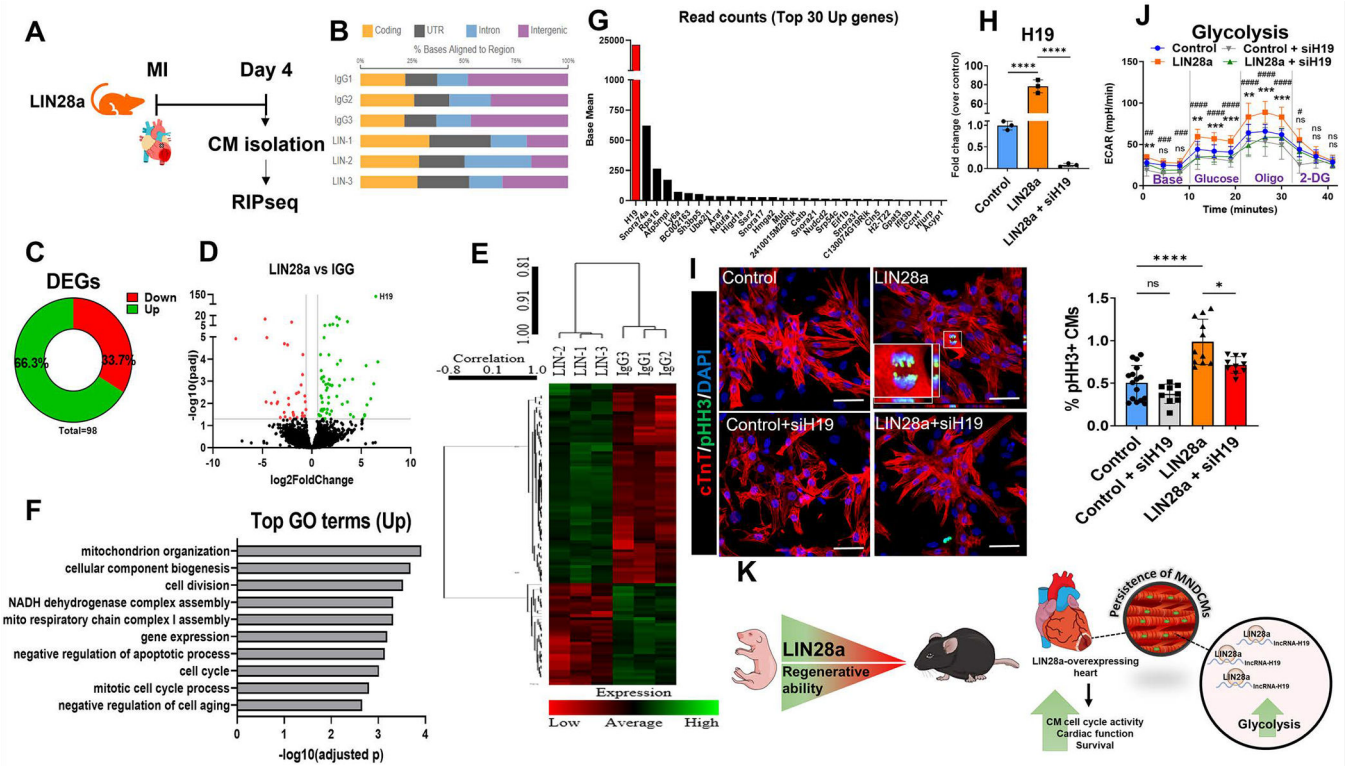

Figure 7: LIN28a binds and regulates expression of long non-coding RNA H19 associated with glycolysis and cell cycle activity in CMs.

A) Schematic of the experimental design. B) Distribution of total nucleotide bases in the reads that map to annotated exons (coding), introns, UTRs, and intergenic regions bases aligned to mRNA regions. C) Pie chart revealing that from the 98 differentially expressed genes, 65 (66.3%) were upregulated while 33 (33.7%) were downregulated. D) Volcano plot resulting from the RIPseq analysis showing upregulated (Green) and downregulated (Red) genes. Genes were considered significant if p-adjusted value < 0.05 after false discovery rate (FDR) test, and differentially expressed if FC > 1.5. n=3 samples per group. E) Clustering analysis and heat map of the 98 differently expressed genes. F) Gene ontology (GO) analysis showing the top over-represented terms of upregulated genes ranked by significance. GO was performed using PANTHER 16.0 classification system. G) Averaged and normalized counts for the top 30 upregulated genes. H) qPCR validation showing H19 mRNA levels are increased in NRVMs 48h after transduction with adenovirus overexpressing LIN28a and downregulated 48h after siH19 treatment. n = 3 independent experiments. I) Analysis of pHH3 indicating LIN28a-induced enhancement in cell cycle activity is diminished in NRVMs overexpressing LIN28a after treatment with 25nM siH19 for 48h. Red=cardiac troponin T, Green=pHH3, Blue=nuclei; scale bar=25μM. n=3 independent experiments. J) Seahorse glycolysis stress test revealing LIN28a-induced enhancement in glycolytic flux is impaired in NRVMs overexpressing LIN28a and treated with 25nM siRNA targeting H19 for 48h. n=3 independent experiments, 12 technical replicates/experiment. K) Schematic illustration of the main findings of the study. Data from H and I was analyzed using Kruskal-Wallis test with Dunn's correction for multiple comparisons; for J, 2way mixed effect ANOVA with Geisser-Greenhouse and Tukey corrections was applied.

Control vs. LIN28a or LIN28a-inhibitor or LIN28a + siH19 *p<0.05, **p<0.01, ***p<0.001, ****p<0.0001, LIN28a vs LIN28a + siH19 #p<0.05, ##p<0.01, ###p<0.001, ####p<0.0001; ns = non-significant.